HHS Public Access

Author manuscript

Nat Genet. Author manuscript; available in PMC 2014 February 28.

Published in final edited form as:

Nat Genet. 2013 September ; 45(9): 1004–1012. doi:10.1038/ng.2715.

Loss of cilia suppresses cyst growth in genetic models of autosomal dominant polycystic kidney disease

Ming Ma[1], **Xin Tian**[1], **Peter Igarashi**[2], **Gregory J. Pazour**[3], and **Stefan Somlo**[1,4,‡]

[1]Department of Internal Medicine Yale University School of Medicine, New Haven, CT, USA

[2]Department of Medicine, University of Texas Southwestern School of Medicine Worcester, MA, USA

[3]Program in Molecular Medicine, University of Massachusetts Medical School, Worcester, MA, USA

[4]Department of Genetics, Yale University School of Medicine, New Haven, CT, USA

Abstract

Kidney cysts occur following inactivation of polycystins in otherwise intact cilia or following complete removal of cilia by inactivation of intraflagellar transport-related proteins. We investigated the mechanisms of cyst formation in these two distinct processes by combining conditional inactivation of polycystins with concomitant ablation of cilia in developing and adult kidney and liver. We found that loss of intact cilia suppresses cyst growth following inactivation of polycystins and that the severity of cystic disease was directly related to the length of time between the initial loss of the polycystin proteins and the subsequent involution of cilia. This cilia-dependent cyst growth was not explained by activation of the MAPK/ERK, mTOR or cAMP pathways and is likely to be distinct from the mechanism of cyst growth following complete loss of cilia. The data establish the existence of a novel pathway defined by polycystin-dependent inhibition and cilia-dependent activation that promotes rapid cyst growth.

Autosomal dominant polycystic kidney disease (ADPKD) is one of the most common potentially lethal human monogenic diseases, affecting over 12 million people worldwide. ADPKD manifests as fluid filled cystic dilation of a small subset of kidney tubules. These cysts result in kidney enlargement that progresses over decades and causes kidney failure in 50% of affected individuals by age 60 [1]. Primary cilia have been identified as the key organelle in the pathogenesis of ADPKD and related cystic diseases[2-4]. In lumen forming epithelia such as the kidney tubules, primary cilia are solitary microtubule-based non-motile projections on the apical surface. They have an overlying plasma membrane but are devoid of subcellular organelles and protein synthetic capacity. Specialized translocation

‡To whom correspondence should be addressed at: Section of Nephrology, Yale University School of Medicine, P.O. Box 208029, 333 Cedar Street, New Haven, CT 06520-8029, USA. Tel: +1 203 737 2974; Fax: +1 203 785 4904; stefan.somlo@yale.edu.

Author Contributions M.M. co-designed the study, performed experiments, co-wrote the manuscript; X.T. performed experiments; P.I. contributed critical reagents and supplementary data; G.J.P. contributed critical reagents; S.S. co-designed the study and wrote the manuscript.

machinery, collectively referred to as intraflagellar transport (IFT), is required to traffic component proteins into and out of cilia[5,6]. Among the many proteins delivered to cilia by IFT are the integral membrane protein products of the genes mutated in ADPKD, polycystin-1 (PC1) and polycystin-2 (PC2)[7-9]. Loss of either polycystin results in ADPKD. Kidney cysts also arise following disruption of cilia by targeted inactivation of genes encoding IFT components such as the heterotrimeric kinesin component Kif3a [10] and the IFT proteins, Ift20 [11] and Ift88 [7,12,13].

It is generally hypothesized that the primary cilium of kidney epithelial cells acts as a sensory organelle and that PC1 and PC2 form a receptor-channel sensory complex in the cilium. Flow has been proposed as the proximate signal being transduced[14,15], although chemosensory inputs have not been excluded[16]. Examination of a diverse array of model systems has implicated a multitude of effector pathways in ciliary and cystic diseases: planar cell polarity, canonical Wnt, mTOR, cAMP, G-protein couple receptor, CFTR, EGF receptor, MAPK/ERK, cellular Ca^{2+}, and cell cycle [reviewed in [4,17-19]]. Nonetheless, the true genetic interrelationship between polycystins and cilia has not been explored leaving open the possibility of divergence between the cellular pathway(s) specifically affected by loss of PC1/PC2 and the pathways affected following loss of structurally intact cilia. In the current study, we combined inactivation of *Pkd1* and *Pkd2* with loss of *Kif3a* and *Ift20* to show that structurally intact cilia are required to promote rapid cyst growth following loss of PC1 or PC2. The data show the existence of signaling pathways that exhibit cilia-dependent activation and polycystin- and cilia-dependent inhibition and that are central to the pathogenesis of ADPKD.

Results

Loss of cilia suppresses cyst growth following inactivation of polycystins

We initially examined the genetic interrelationship between cyst formation resulting from inactivation of polycystins or cilia or both. We used the collecting duct selective *Pkhd1-cre* [20,21] in combination with the conditional alleles $Pkd1^{fl}$ [22], $Pkd2^{fl}$ [21], $Kif3a^{fl}$ [10] and $Ift20^{fl}$ [11]. Reporter gene studies showed Cre activity in ~100% of collecting duct cells by P7 (Supplementary Note; Supplementary Fig. 1) with complete disappearance of cilia by P11 in *Pkhd1-cre;* $Kif3a^{fl/-}$ mice and by P18 in *Pkhd1-cre;* $Ift20^{fl/-}$ mice (Supplementary Note; Supplementary Fig. 2). The delayed disappearance of cilia results from differences in the rate of disappearance of the respective proteins and dynamics of cilia disassembly following gene inactivation. *Pkhd1-cre;* $Kif3a^{fl/-}$ and *Pkhd1-cre;* $Ift20^{fl/-}$ mice show only mild cyst formation at P24 (Fig. 1a-h). *Pkhd1-cre;* $Pkd1^{fl/fl}$ and *Pkhd1-cre;* $Pkd2^{fl/fl}$ mice exhibit severe cystic disease at the same age (Fig. 1a-h). Unexpectedly, inactivation of *Pkd1* or *Pkd2* concomitantly with *Kif3a* or *Ift20*, respectively, results in intermediate polycystic disease severity (Fig. 1a-h). The reduced severity of the polycystic phenotype in double mutants compared to polycystin single mutants is apparent using aggregate data on kidney weight-to-body weight ratio, percentage of cystic area and serum urea nitrogen (Fig. 1b, f; Supplementary Fig. 3). Immunocytochemistry confirmed the presence of cilia in cysts in polycystin single mutants (Fig. 1d, h) and absence cilia in cysts in double mutants (Fig. 1c, g).

The beneficial effect of loss of cilia on cyst formation due to ADPKD gene mutations was independent of the Cre recombinase transgenic line used and was present at earlier time points (Supplementary Figs. 4, 5). We also considered whether the relatively mild cyst formation in the cilia-only mutants is the result of a suppressive effect from persistent expression of PC1 at cellular sites outside cilia. We tested this by either reducing the gene dosage of *Pkd1* in *Ksp-cre; Kif3a*$^{fl/fl}$*; Pkd1*$^{fl/+}$ mice or increasing *Pkd1* dosage using a three-copy *Pkd1*$^{F/H}$*-BAC* transgene[23] in *Ksp-cre; Kif3a*$^{fl/fl}$*; Pkd1*$^{F/H}$*-BAC* mice. Reduced *Pkd1* dosage did not result in increased severity of cysts and increased *Pkd1* dosage did not show reduced cyst formation compared to *Ksp-cre; Kif3a*$^{fl/fl}$ mice (Supplementary Fig. 6). These findings suggest that the severity of cyst progression following loss of *Pkd1* or *Pkd2* alone is dependent on the presence of intact cilia, but that cyst progression following loss of cilia alone is independent of polycystin function.

Intact cilia devoid of polycystins are required for rapid cyst growth

One implication of the interdependence of polycystins and cilia in cyst formation is that the longer the period during which intact cilia persist after loss of polycystins, the greater the severity of cyst formation. We tested this mechanism directly by varying interval between polycystin and cilia loss (Fig. 2). *Kif3a*$^{fl/fl}$ mice have a higher initial level of Kif3a protein compared to the *Kif3a*$^{fl/-}$ mice (Fig. 2a) resulting in delayed disappearance of cilia in *Pkhd1-cre; Kif3a*$^{fl/fl}$ kidneys (P14) compared to *Pkhd1-cre; Kif3a*$^{fl/-}$ kidneys (P11; Supplementary Fig. 2c, d). We generated age-matched P24 *Pkhd1-cre; Kif3a*$^{fl/fl}$ mice and compared kidney cyst disease progression with the *Pkhd1-cre; Kif3a*$^{fl/-}$ mice shown in Fig. 1a, b. *Pkhd1-cre; Kif3a*$^{fl/fl}$ mice had reduced cystic index compared to *Pkhd1-cre; Kif3a*$^{fl/-}$ mice suggesting that the later loss of cilia in the *Pkhd1-cre; Kif3a*$^{fl/fl}$ cilia-only mutant mice delayed the onset of cyst growth (Fig. 2b, c; Supplementary Fig. 3). Comparison of *Pkhd1-cre; Kif3a*$^{fl/fl}$*; Pkd1*$^{fl/fl}$ mice at P24 with the *Pkhd1-cre; Kif3a*$^{fl/-}$*; Pkd1*$^{fl/fl}$ from Fig. 1a, b showed that the same delay in loss of cilia in the cilia-polycystin double knockout had the opposite effect, increasing the severity of cysts (Fig. 2b, c; Supplementary Fig. 3). We next tested this mechanism in the opposite direction by decreasing the germ line dosage of PC2. Reduced basal levels of PC2 (Fig. 2d), resulting in earlier disappearance of the protein following Cre-mediated gene inactivation, gives rise to increased cyst severity in *Pkhd1-cre; Pkd2*$^{fl/-}$ mice compared to the *Pkhd1-cre; Pkd2*$^{fl/fl}$ mice (Fig. 2e, f). In the setting of invariant timing of cilia loss on the *Kif3a*$^{fl/fl}$ background, *Pkhd1-cre; Kif3a*$^{fl/fl}$*; Pkd2*$^{fl/-}$ mice, with a prolonged interval between PC2 and cilia loss, showed more severe polycystic disease compared to *Pkhd1-cre; Kif3a*$^{fl/fl}$*; Pkd2*$^{fl/fl}$ mice (Fig. 2e, f).

We were able to complement the genetic data to show that loss of polycystin protein antecedes involution of cilia in our models. We selected time points P7, P10, P15 to evaluate the course of PC2 and cilia loss in collecting ducts of *Pkhd1-cre; Kif3a*$^{fl/fl}$*; Pkd2*$^{fl/fl}$ double mutant mice (Fig. 2g-l). Control mice have intact cilia that express PC2 (Fig. 2g, k). At P7 double knockout mice have intact cilia that either do not express PC2 (arrows) or express very little PC2 (arrowhead) when compared to tubule segments in which *Pkhd1-cre* was not active (Fig. 2h, i). At P10, intact cilia remain but are completely devoid of PC2 (Fig. 2j). At P15, cilia are no longer present in the double knockouts (Fig. 2l). The immunofluorescence data show that cilia without polycystin are present by P7 and persist through P14 after which

cilia are no longer present. PC1 cannot be detected by immunofluorescence in a manner similar to PC2. PC1 is a lower abundance protein than PC2 and its dosage that is rate limiting in cyst formation[23], so it is reasonable to extrapolate that PC1 disappears from cilia even earlier than PC2. This longer period during which cilia are present without polycystin results in more severe cystic changes (compare *Kif3a*$^{fl/fl}$*;Pkd1*$^{fl/fl}$ in Fig. 2b, c to *Kif3a*$^{fl/fl}$*;Pkd2*$^{fl/fl}$ in Fig. 2e, f). The data support the hypothesis that intact cilia elaborate a positive signal for rapid cyst growth that is normally inhibited by polycystin action. The activity of this cyst promoting signal requires structurally preserved cilia and is maximally active when cilia are devoid of polycystins, as is the case in ADPKD.

Cilia-polycystin double mutants ameliorate adult onset polycystic disease

The course of ADPKD is substantially slower in adult mice following conditional inactivation of polycystins or cilia[13,24]. We next determined whether cilia ablation is beneficial in the more indolent adult forms of polycystic kidney disease using the kidney selective whole nephron bi-allelic *Pax8*^{rtTA}*; TetO-cre* doxycycline-inducible system[25] (Fig. 3). We induced mice with oral doxycycline from P28-P42 and determined the pattern of cre reporter gene activity along the nephron and the timing of cilia loss (Supplementary Note; Supplementary Fig. 7). There was minimal cyst formation 8 weeks after the start of induction in both *Pax8*^{rtTA}*; TetO-cre; Pkd1*$^{fl/fl}$ single mutant and *Pax8*^{rtTA}*; TetO-cre; Kif3a*$^{fl/fl}$*; Pkd1*$^{fl/fl}$ double mutant kidneys (Fig, 3a, b). Nonetheless, *Pax8*^{rtTA}*; TetO-cre; Pkd1*$^{fl/fl}$ single mutant kidneys already showed increased kidney-to-body weight ratio and increased cystic index primarily due to early cortical nephron cyst formation (Fig, 3a, b). These differences became profoundly manifest 14 weeks after the start of doxycycline induction with *Pax8*^{rtTA}*; TetO-cre; Kif3a*$^{fl/fl}$*; Pkd1*$^{fl/fl}$ double mutant kidneys remaining indistinguishable from wild type mice while *Pax8*^{rtTA}*; TetO-cre; Pkd1*$^{fl/fl}$ single mutants showed marked cyst progression and significant renal functional impairment (Fig, 3c, d). Similar results were obtained with *Kif3a;Pkd2* double knockouts compared to *Pkd2* single knockouts (Supplementary Fig. 8).

We evaluated the temporal relationship between loss of the polycystin and Kif3a proteins in these adult onset mouse models. Immunoblotting of kidney tissue lysates at 1, 2 and 3 weeks after the start of doxycycline showed that PC2 levels were already significantly reduced 1 week after starting doxycycline while Kif3a levels required a longer time to show comparable changes in expression (Fig. 3e). Immunofluorescence studies similarly showed that PC2 disappeared from cilia well before cilia disappeared in *Kif3a;Pkd2* double mutant kidney tubules. PC2 was detected in kidney tubule cell cilia from control mice (Fig. 3f) and *Pkd2* single mutant mice (Fig. 3g) and *Kif3a;Pkd2* double mutant mice (Fig. 3h) 1 week after start of doxycycline. By 11 days after starting doxycycline, cilia persisted but were devoid of PC2 in *Kif3a;Pkd2* double mutant mice (Fig. 3h). Cilia became sparse at 2 weeks and were completely absent at 3 weeks after start of doxycycline (Fig. 3h). Liver cysts are part of the ADPKD phenotype in man. We used the tamoxifen-inducible *UBC-cre*^{ER} [26] to show that cilia ablation also markedly slows bile duct derived cyst growth and has durable effects on kidney cyst growth in *Pkd1* models (Supplementary Note; Supplementary Figs. 9. 10). Cyst growth pathways dependent on intact cilia are the fundamental mechanism underlying all kidney and liver cyst formation due to mutations in *Pkd1* and *Pkd2*

irrespective of tissue or cell type or age of cyst initiation. Polycystic kidney and liver disease can be markedly slowed by inhibiting this cilia-dependent pathway, for example, by ablating cilia.

Intact cilia result in higher rates of proliferation following loss of polycystins

Cyst growth manifests with increased proliferation of cells that have lost polycystin expression[22,23]. We determined whether the beneficial effect of concomitant loss of cilia was the result of a decrease in this proliferative response or another mechanism such as increased apoptosis of cyst cells. We quantitated the rate of nephron segment-specific cyst cell proliferation by determining the proportion of Ki67- or BrdU-positive nuclei. Collecting duct cysts marked by lectin Dolichos biflurous agglutinin (DBA) in early onset *Pkhd1-cre* models showed ~1% proliferation in *Kif3a* single mutants when determined by either BrdU incorporation or Ki67 staining (Fig. 4a-d). Polycystin single mutants based on either *Pkd1* or *Pkd2* showed ~5% proliferation in collecting duct cyst cells (Fig. 4a-d). The rates of proliferation in the cilia-polycystin double mutants were significantly reduced compared to the respective polycystin-only mutants and correlated with relative cyst severity in early onset *Pkhd1-cre*-based models (Fig. 4a-d).

We next examined segment specific rates of proliferation following inactivation by *Pax8^{rtTA}; TetO-cre* in proximal tubules marked by lotus tetragonolobus agglutinin (LTA) and in collecting ducts marked by DBA at 8 and 14 weeks after the start of doxycycline induction. Consistent with the slower rate of cyst growth, the absolute rates of proliferation were lower in the adult inducible model compared to the early onset *Pkhd1-cre* model. Nonetheless, proliferation rates in proximal tubules and collecting ducts were elevated in the *Pkd1* single knockouts compared to wild type controls (Fig. 4e-h). The proliferation rates in both segments appeared higher at 14 weeks than 8 weeks, suggesting that cyst growth rates may not be constant and there may be amplification of the proliferative signal with progressive polycystic disease. Proliferation rates in cilia-*Pkd1* double knockouts were indistinguishable from wild type (Fig. 4e-h), recapitulating the absence of phenotypic differences between these genotypes (Fig. 3). Reduced proliferation in cilia-polycystin double mutants was also found in the tamoxifen inducible *UBC-cre^{ER}* adult onset model (Supplementary Fig. 10). There were no differences in the rates of apoptosis as determined by TUNEL in any of these models (data not shown). The severity of polycystic disease is correlated with increased rates of cyst cell proliferation which are at least in part dependent on the presence of intact cilia.

A novel cilia-dependent cyst activating mechanism

We next sought to evaluate whether known signaling pathways implicated in the pathogenesis of ADPKD exhibited features of cilia dependence that would make them candidates for the novel polycystin inhibited, cilia-dependent proliferative cyst promoting pathway. To this end, we examined the activity of the mitogen activate protein kinase/ extracellular signal related kinase (MAPK/ERK), mammalian target of rapamycin (mTOR), and cyclic adenosine monophosphate (cAMP) pathways[27-29]. These pathways have shown activity in mice with established cystic disease and have been the targets of both preclinical and clinical therapeutic interventions.

We used the adult onset models based on *Kif3a*, *Pkd1* and *Pax8^{rtTA}; TetO-cre* at 8 and 14 weeks after start of induction with doxycycline. To determine MAPK/ERK activation, we examined the levels of phosphorylated ERK1/2 (phospho-ERK) in whole kidney lysates by semi-quantitative immunoblotting (Fig. 5a, b)[22]. There were no differences in levels of phospho-ERK based on genotype at 8 weeks after doxycycline (Fig. 5a). At 14 weeks, *Pax8^{rtTA}; TetO-cre; Pkd1$^{fl/fl}$* single mutants showed significantly increased phospho-ERK expression; *Pax8^{rtTA}; TetO-cre; Kif3a$^{fl/fl}$; Pkd1$^{fl/fl}$;* double mutants did not differ from wild type (Fig. 5b). Immunohistochemistry in kidneys at 14 weeks showed that phospho-ERK was expressed in collecting ducts irrespective of genotype suggesting that at least some of the increase in phospho-ERK in cystic kidneys was related to increased cell mass of this segment as a result of cyst progression (Fig. 5c). The cystic *Pax8^{rtTA}; TetO-cre; Pkd1$^{fl/fl}$* single mutants also had increased phospho-ERK in thick ascending loop of Henle, and this appeared to be a feature of progressive polycystic disease (Fig. 5c, *bottom panels*). Phospho-ERK was uniformly absent from proximal tubules in all genotypes irrespective of the presence of cysts (Fig. 5c). These results are notable for two observations. First, the absence of increased phospho-ERK at 8 weeks when early cyst formation and increased proliferation are already manifest in *Pax8^{rtTA}; TetO-cre; Pkd1$^{fl/fl}$* single mutants (Fig. 3a,b; Fig. 4 e-h) suggests that the earliest stages of cyst growth following loss of PC1 are not associated with MAPK/ERK pathway activation. Second, the complete absence of any phospho-ERK activation even in late stage and markedly cystic *Pax8^{rtTA}; TetO-cre; Pkd1$^{fl/fl}$* proximal tubules indicates that MAPK/ERK activation is not a ubiquitous contributor to cyst growth in ADPKD. Taken together, the data make it unlikely that the MAPK/ERK mediated pathways are responsible for the generalized cyst growth signal dependent on intact cilia following inactivation of *Pkd1*.

Abnormal activation of mTOR has been implicated in ADPKD[30,31] and tied to cilia function[15,32]. mTOR inhibitors were among the first agents tried in large scale clinical trials with ADPKD patients[33,34]. We evaluated mTOR activation by assaying phosphorylation of a downstream target, S6 ribosomal protein (S6RP), using semi-quantitative immunoblotting of kidney lysates. We verified the specificity of the antibodies to detect decreased phospho-S6RP following down-regulation of mTOR in the setting of serum starvation (Fig. 5d). We found no discernible differences in phospho-S6RP in kidney tissue lysates from wild type, *Pkd1*-only and cilia-*Pkd1* double mutant kidneys at either 8 or 14 weeks following the start of gene inactivation (Fig. 5e, f). mTOR activation does not appear to be a major contributor to ADPKD in adult inducible whole nephron knockout of *Pkd1* irrespective of the presence or absence of intact cilia.

Elevated levels of cAMP are present in animal models of PKD[35,36] and foster the growth of kidney cysts[37,38]. cAMP regulates expression of target genes in part through the protein kinase-A-mediated phosphorylation at Ser133 of the transcription factor cAMP response element-binding protein (CREB). We evaluated cAMP activity in the adult models of ADPKD by semi-quantitative immunoblotting in cytoplasmic and nuclear fractions of kidney tissue lysates and by immunohistochemistry (Fig. 5g-i). We confirmed the specificity of the anti-phospho-CREB antibodies for immunoblotting and immunocytochemistry by examining cells following activation of cAMP with forskolin (Supplementary Fig. 11).

Fractionation of kidney lysates showed that CREB and phospho-CREB were enriched in nuclear fractions (Fig. 5g, h). Levels of nuclear phospho-CREB elevated above baseline were seen at 8 and 14 weeks, but only in *Pax8^{rtTA}; TetO-cre; Pkd1$^{fl/fl}$* single mutants. *Pax8^{rtTA}; TetO-cre; Kif3a$^{fl/fl}$;Pkd1$^{fl/fl}$* double mutants did not show evidence of cAMP activation above the wild type baseline (Fig. 5g, h). Immunohistochemical analysis of phospho-CREB expression in kidney sections showed increased nuclear expression in cyst lining cells (Fig. 5i). As was the case with MAPK/ERK activation, cAMP activation was confined to distal nephron segments and completely absent from proximal tubules regardless of genotype or cyst burden (Fig. 5i). Since cilia ablation is effective in ameliorating cyst growth in all segments, including the proximal tubule, the absence of cAMP activation in proximal tubule cysts suggests that cAMP is not fundamental to the cilia-dependent cyst growth pathway activity following loss of *Pkd1*. The aggregate genetic data point to a novel cyst promoting pathway dependent on intact cilia devoid of functional polycystins that may be an ideal therapeutic target for treatment of ADPKD.

Discussion

We define a novel and unexpected relationship between integrity of cilia structure and polycystin function—the existence of a cilia-dependent cyst growth promoting pathway that specifically effects cyst growth dependent on the presence of intact cilia devoid of either PC1 or PC2. This pathway activity determines cyst progression following both early and late ADPKD gene inactivation, is equally applicable to polycystic kidney and polycystic liver disease and is active in cyst growth in all nephron segments. None of the pathways implicated in the pathogenesis of ADPKD to date, save PC1 and PC2 themselves, have achieved this degree of universality in determining the phenotype. The success of cilia ablation in reducing cyst growth irrespective of the timing or tissue of polycystin gene inactivation suggests that differences within orthologous gene models of ADPKD, e.g., early vs. late inactivation, are more differences in degree than differences in fundamental mechanism. A common therapeutic strategy should be effective in ADPKD regardless of the timing or tissue of cyst formation.

The mechanism of cystic disease in cilia-polycystin dual inactivation models is a function of the duration of the interval between the early disappearance of polycystins and the subsequent involution of cilia. In polycystin-only mutants this interval is indefinite. Our studies leave open the possibility that medicinal inhibition of the cilia-dependent pathway can slow cyst growth even when applied at times significantly after loss of polycystin. MAPK/ERK, mTOR and cAMP effectors are unlikely to be the central to the cilia-dependent signal largely because they show restricted nephron segment specificities and later activation. That is not to say that these pathways are not indirectly activated in certain cell types or conditions to actively promote cyst growth. It is rather to suggest that the cilia-dependent pathway is a more proximate and universally applicable target for reducing cyst growth. While cyst growth following loss of polycystins is cilia-dependent, cyst growth following loss of cilia may be polycystin-independent. Loss of cilia alone results in relatively slower cyst growth and neither concomitant reduction in dose nor overexpression of PC1 appears to significantly impact this process *in vivo*.

Our earlier studies have shown that the polycystin functions are continuously regulated trait in which decreases in polycystin signaling result in graded increases in tubule luminal morphologies, ultimately leading to cysts when polycystin signaling falls below a critical threshold[23]. The current study shows that PC1/PC2 input inhibits a signal dependent on intact cilia and complete loss this inhibition gives rise to cysts. This signal is unlikely to be a primary proliferation effect as occurs with neoplasia since cyst growth requires only low level proliferation and cells retain differentiated properties. Increased proliferation in cysts is detectable when examined specifically in cells in which cre recombinase is active, but it is below detection as a differential signal when whole kidney proliferation is evaluated[24]. The proliferation in cysts is an inherent effect of the polycystin-inhibited, cilia-dependent cyst growth signal, as recent studies have shown that exogenous proliferative signals do not promote cyst growth following loss of cilia[39]. It likely that the normal physiologic roles of PC1/PC2 subsume controlled derepression of this cilia pathway promoting functional tubule adaptation to either chemical or mechanical signals.

Loss of function mutations in components of the cilia-dependent pathway would not result in cysts and would require a cyst suppressor screen to be discovered in model organisms. Given that we were able to discover dominantly inherited gene mutations for isolated human polycystic liver disease that phenocopy ADPKD by acting indirectly on biogenesis of polycystins[23], we expect the human phenotype to be sensitive enough to find other genes in which heterozygous loss of function alleles result in ADPKD. The absence of a third gene for ADPKD supports the inhibitory roles of polycystins in a pathway whose other components are constitutively activating. The potential complexities of the relationship between polycystin function and cilia structure is illustrated by the roles for cilia in Hedgehog (Hh) dependent tumorigenesis pathways[40,41]. Hh ligand binds to Patched (Ptch) on cilia thereby relieving repression of Smoothened which enters the cilium and promotes translocation of transcription activators Gli1 and Gli2 from cilia to the nucleus[42]. Removal of cilia inhibits Hh ligand-dependent carcinomas but perturbs the balance between the activating factors and Gli3 repressor, thereby promoting tumor growth under conditions mimicking downstream activation of Hh signaling[40,41]. The prevailing view of the cyst-suppressive role of polycystins is that it requires either mechanical or ligand activation to effect calcium dependent inhibition of cyst growth[14,16,43]. The current findings suggest that in a manner analogous to the role of Ptch, polycystins provide a tonic, flow or ligand independent suppressive signals for a cilia-dependent signal. In this case, flow or ligand may decrease this inhibition in a regulated manner as part of a normal physiological or homeostatic cilia-dependent signal. Complete loss of polycystins results in constitutive activation of the cilia-dependent cyst promoting signal, just as ligand-independent Hh signaling occurs in Ptch knockouts[44].

Although our studies were not able to directly prove it, they strongly suggest that that the components of cilia-dependent cyst signals are present in cilia, in a manner to the components of Hh signaling. The next steps in the molecular definition of this cilia-dependent pathway will require new strategies directed at discovery of intra-cilial signaling complexes whose loss of function suppresses polycystic disease following inactivation of polycystins. Our *in vivo* studies serve as a proof-of-principle that discovery and targeting of

the cilia-dependent, polycystin-inhibited pathway will be effective in slowing the course of ADPKD. We propose that the novel cilia-dependent pathway is the central biological mechanism for polycystin and cilia signaling in ADPKD. Elucidation of the components of pathway will define superior targets with a high likelihood for translation into therapies for this disease.

Online Methods

Mouse strains and histology

The mouse strains used in the current study have been previously described: *Pkd1*^{fl} [22], *Pkd2*^{fl} [21], *Pkd2*$^{-}$ [45], *Pkd1*$^{F/H}$*-BAC* [23], *Kif3a*^{fl} [46,47], *Ift20*^{fl} [11], *Pax8*^{rtTA} [25], *TetO-cre* [48], *Pkhd1-cre* [20], *Ksp-cre* [49], *UBC-cre*^{ER} [26], *ROSA*$^{mT/mG}$ [50] and *Rosa*^{lacZ} [51]. They are predominantly on a C57Bl/6 genetic background.

Pax8^{rtTA}; *TetO-cre* mice were induced with 2 mg/ml doxycycline (Sigma-Aldrich, St Louis, Missouri) in drinking water supplemented with 3% sucrose for 2 weeks from P28 to P42. Mice were sacrificed at 1 week, 11 days, 2 weeks, 3 weeks, 25 days, 8 weeks and 14 weeks after the start of induction. One kidney was snap-frozen and the other kidney was fixed in 4% PFA for histological analysis; for immuno-fluorescence of PC2, one kidney was perfusion-fixed with PLP fixative (lysine, 0.075 M; disodium phosphate, 0.0375M; sodium periodate, 0.01M; paraformaldehyde, 2%; pH7.4). *UBC-cre*^{ER} mice were induced with Tamoxifen (Sigma) delivered by intraperitoneal injection at a dose of 2 mg daily from P28 to P32. Mice were sacrificed at 12 and 20 weeks after the end of tamoxifen treatment. Sagittal sections of kidneys were processed for hematoxylin and eosin staining and cystic index was calculated as previously reported[22].

All animals were used in accordance with scientific, humane, and ethical principles and in compliance with regulations approved by the Yale University Institutional Animal Care and Use Committee.

Immunofluorescence

The following antibodies and lectins were used: Mouse monoclonal anti-BrdU (Sigma); rabbit anti-Ki67 (Vectors Laboratories, Burlingame, California); FITC or rhodamine conjugated-*Dolichos biflorus agglutinin* (DBA, Vectors Laboratories); rhodamine-*Lotus tetragonolobus agglutinin* (LTA, Vectors Laboratories); anti-megalin[52]; goat anti-aquaporin-2 (Santa Cruz Biotechnology, Santa Cruz, California); rabbit-anti-phospho-MAPK/ERK1/2, rabbit-anti-phospho-CREB (Cell Signaling and Technology, Danvers, Massachusetts); rabbit-anti-PC2 (YCC2)[53]; mouse-anti-α-acetylated-α-tubulin (Sigma); rabbit anti-Arl13b[54]; sheep-anti-THP (Tamm-Horsfall protein, Biotrend Chemicals, Destin, Florida); mouse-anti-Calbindin (Sigma); Alex-488, Alex-594 and Alex-647 conjugated secondary antibodies (Molecular Probes). Hoechst 33342 (Molecular Probes) was used for nuclear staining. Images were taken under Nikon Eclipse TE2000-U microscope under the control of MetaMorph software (Universal Imaging).

Proliferation and apoptosis

Proliferation was measured by Ki67-positive or BrdU-positive nuclei. For BrdU incorporation, mice received 100 μl of 5-bromo-2′-deoxyuridine (BrdU, 10 mg/ml, BD Pharmigen, San Jose, California) by intraperitoneal injection 3 hours before sacrifice. Kidneys were fixed with 4% PFA overnight and embedded in OCT after 30% sucrose infiltration and processed for immunofluorescence. The numbers of Ki67-positive or BrdU-positive were counted in at least 1000 DBA or LTA positive nuclei per animal. Apoptosis was determined using the *in situ* Cell Death Detection kit (Roche, Basel, Switzerland) TUNEL method according to the manufacturer's manual and counted in the same manner as proliferation markers.

Immunoblotting and quantitation by densitometry

Frozen whole kidneys were homogenized with Hanoka's IP buffer (NaCl 150 mM, NaH_2PO_4 20 mM, glycerol 10%, Triton X-100 0.5%) supplemented with complete EDTA-free protease inhibitor cocktail tablets (Roche) and PhosSTOP phosphatase inhibitor cocktail tablets (Roche). Lysates were centrifuged for 3,000 rpm at 4°C. Protein concentrations were measured with Protein Assay Dye Reagent Concentrate (Bio-Rad, Hercules, California). Equal amounts of total protein were loaded and separated in 4-20% Mini-Protean TGX Precast Gels (Bio-Rad) and transferred to PVDF transfer Membrane (PerkinElmer). Membranes were sequentially incubated with primary antibodies overnight at 4°C after 1 hour blocking with 5% milk. Primary antibodies used: anti-phospho-MAPK/ERK1/2, MAPK/ERK1/2, anti-phospho-S6RP, anti-S6RP (Cell Signaling and Technology); anti-KIF3a (Abcam) were used at dilution of 1:1000; rabbit-anti-PC2 (YCC2)[53]; rabbit-anti-phospho-CREB, rabbit-anti-CREB (Cell Signaling and Technology); goat-anti-LaminA/C (Santa Cruz Biotechnology); rabbit-anti-calnexin (Enzo Life Sciences); rabbit anti-HSP90 (Santa Cruz Biotechnology); anti-GAPDH (Cell Signaling and Technology) were used at 1:5000. Secondary antibodies anti-rabbit-Hrp (1:5000) and anti-mouse-Hrp (1:5000) (Jackson ImmunoResearch Laboratories) were incubated with the membrane for 1 hour. Western Lightning Plus-ECL (PerkinElmer) was used for chemi-luminescence detection. The volume of individual immunoblot bands, in pixels, was determined by optical densitometry using ImageQuant software (Molecular Dynamics).

Validation of phospho-S6RP antibody

70% confluent immortalized mouse kidney tubule epithelial cells (PH2) were incubated with DMEM:F12 plus 5% FBS or DMEM:F12 alone for 17 hours at 37°C. Cells were digested with lysis buffer supplemented with complete protease inhibitor and PhosSTOP (Roche) and proteins were extracted and immunoblotted as above.

Validation of phosphor-CREB antibody

70% confluent immortalized mouse kidney tubule epithelial cells (PH2) were incubated with DMEM:F12 or DMEM:F12 supplemented with 100 μM forskolin (Sigma) dissolved in DMSO or DMSO alone for 30 minutes at 37 °C. Cells were fixed with 4% PFA for immunofluorescence or digested with lysis buffer for immunoblotting.

Kidney nuclear fractionation

Kidney non-nuclear and nuclear extract preparation was performed as previously reported[55] with slight modifications. All buffers (NB1-NB5) were supplemented with complete protease inhibitor and PhosSTOP phosphatase inhibitor (Roche). Kidneys were rinsed with ice cold PBS, and were homogenized in 0.3 ml of NB1 buffer (10 mM Tris, pH 8.0, 10 mM NaCl, 3 mM MgCl2, 0.5 mM DTT, 0.1% Triton X-100, 0.1 M sucrose) using 2ml Dounce homogenizer (Wheaton). Homogenates were gently mixed with 0.3 ml NB2 buffer (NB1 with 0.25 M sucrose) and the homogenate after NB1 and NB2 mixing were filtered through 40 μm cell strainer (BD Biosciences) to remove less well homogenized tissues. 0.5 ml NB3 (10 mM Tris, pH 8.0, 5 mM MgCl2, 0.5 mM DTT, 0.33 M sucrose) was layered under the cell suspension and centrifuged at 1,000 *g* at 4 °C for 10 min. The supernatants contain non-nuclear extracts and the pellets contain nuclear extracts. The non-nuclear extracts were centrifuged at 12,000 *g* for 30 minutes and the supernatant soluble proteins from non-nuclear extracts were concentrated in a vacuum dryer. The nuclear pellets were washed with NB4 buffer (20 mM HEPES, pH 7.9, 25% glycerol, 1.5 mM MgCl2, 0.2 mM EDTA, 0.5 mM DTT) and re-suspended in NB5 buffer (NB4 with 0.42 M NaCl) under slow rotation for 1 hour at 4°C. The nuclear suspension were clarified by centrifuged for 30 minutes at 12,000 *g* and the supernatants containing solubilized nuclear proteins and processed for immunoblotting.

Serum urea nitrogen analysis

Mice were euthanized and blood were collected by ventricular puncture. Sera were separated using Plasma Separator Tubes with Lithium Heparin (BD). Serum urea nitrogen was analyzed by Mouse Metabolic Phenotyping Center at Yale University.

Sample size and power calculation and statistics

Sample size and power calculations were performed using STPLAN (ver. 4.5; University of Texas, M. D. Anderson Cancer Center). Calculations were based on the following: Each *Pkhd1-cre*; *Pkd1*$^{fl/fl}$ kidney at P24 weighs 0.65 g (S.D. ± 0.15 g) based on our empirical data. Our alternative hypothesis was that loss of cilia in polycystin/cilia double mutant kidneys would result in 40% decrease in kidney weight to 0.40 g (S.D. ± 0.15 g) with a significance level (alpha) of 0.05 (two sided). Under these expectations, 6 mice could achieve 89.9% power, and 7 mice could achieve 95.3% power to detect the difference of 0.25 g between the null hypothesis and the alternative hypothesis. The allocation of animals to each group was solely based on genotype irrespective of gender and without any exclusions.

Data were analyzed by the Mann-Whitney Test or One-Way Analysis of Variance followed by Tukey's multiple comparison test with Graphpad Prism 5 software. The Brown-Forsythe test or Bartlett's test was used to test for equality of group variances. A value of $P < 0.05$ was considered significant. All data are presented as mean (±SEM).

Supplementary Material

Refer to Web version on PubMed Central for supplementary material.

Acknowledgements

We are grateful to Deren Shao and Sue Ann Mentone for assistance with tissue histology; Drs. Kathryn Anderson and Tamara Caspary for anti-Arl13b antibody; Dr. Peter Aronson for forskolin; Dr. Eric Brown for Ubc^{CreER} transgenic mice; the Yale Mouse Metabolic Phenotyping Center for serum urea nitrogen measurement, Core resources from the Yale O'Brien Kidney Center (P30 DK079310) for support with BAC transgenic lines and the Center for Polycystic Kidney Disease Research at Yale (P30 DK090744) for mouse lines. We thank Drs. Yiqiang Cai, Sorin Fedeles, Rachel Gallagher, Zhiheng Yu and Xiangyu Cong for helpful discussions. This work was supported by NIH/NIDDK grants R01 DK54053, RC1 DK086738 and R01 DK51041 (S.S.).

References

1. Grantham JJ, Mulamalla S, Swenson-Fields KI. Why kidneys fail in autosomal dominant polycystic kidney disease. Nat.Rev.Nephrol. 2011
2. Gerdes JM, Davis EE, Katsanis N. The vertebrate primary cilium in development, homeostasis, and disease. Cell. 2009; 137:32–45. [PubMed: 19345185]
3. Sharma N, Berbari NF, Yoder BK. Ciliary dysfunction in developmental abnormalities and diseases. Curr Top Dev Biol. 2008; 85:371–427. [PubMed: 19147012]
4. Hildebrandt F, Benzing T, Katsanis N. Ciliopathies. The New England journal of medicine. 2011; 364:1533–1543. [PubMed: 21506742]
5. Pedersen LB, Rosenbaum JL. Intraflagellar transport (IFT) role in ciliary assembly, resorption and signalling. Curr Top Dev Biol. 2008; 85:23–61. [PubMed: 19147001]
6. Jin H, et al. The conserved Bardet-Biedl syndrome proteins assemble a coat that traffics membrane proteins to cilia. Cell. 2010; 141:1208–1219. [PubMed: 20603001]
7. Yoder BK, Hou X, Guay-Woodford LM. The polycystic kidney disease proteins, polycystin-1, polycystin-2, polaris, and cystin, are co-localized in renal cilia. J.Am.Soc.Nephrol. 2002; 13:2508–2516. [PubMed: 12239239]
8. Pazour GJ, San Agustin JT, Follit JA, Rosenbaum JL, Witman GB. Polycystin-2 localizes to kidney cilia and the ciliary level is elevated in orpk mice with polycystic kidney disease. Curr.Biol. 2002; 12:R378–R380. [PubMed: 12062067]
9. Huang K, et al. Function and dynamics of PKD2 in Chlamydomonas reinhardtii flagella. J Cell Biol. 2007; 179:501–514. [PubMed: 17984324]
10. Lin F, et al. Kidney-specific inactivation of the KIF3A subunit of kinesin-II inhibits renal ciliogenesis and produces polycystic kidney disease. Proc.Natl.Acad.Sci.U.S.A. 2003; 100:5286–5291. [PubMed: 12672950]
11. Jonassen JA, San AJ, Follit JA, Pazour GJ. Deletion of IFT20 in the mouse kidney causes misorientation of the mitotic spindle and cystic kidney disease. J Cell Biol. 2008; 183:377–384. [PubMed: 18981227]
12. Haycraft CJ, Swoboda P, Taulman PD, Thomas JH, Yoder BK. The C. elegans homolog of the murine cystic kidney disease gene Tg737 functions in a ciliogenic pathway and is disrupted in osm-5 mutant worms. Development. 2001; 128:1493–1505. [PubMed: 11290289]
13. Davenport JR, et al. Disruption of intraflagellar transport in adult mice leads to obesity and slow-onset cystic kidney disease. Curr.Biol. 2007; 17:1586–1594. [PubMed: 17825558]
14. Nauli SM, et al. Polycystins 1 and 2 mediate mechanosensation in the primary cilium of kidney cells. Nat.Genet. 2003
15. Boehlke C, et al. Primary cilia regulate mTORC1 activity and cell size through Lkb1. Nat.Cell Biol. 2010; 12:1115–1122. [PubMed: 20972424]
16. Tanaka Y, Okada Y, Hirokawa N. FGF-induced vesicular release of Sonic hedgehog and retinoic acid in leftward nodal flow is critical for left-right determination. Nature. 2005; 435:172–177. [PubMed: 15889083]
17. Harris PC, Torres VE. Polycystic kidney disease. Annual review of medicine. 2009; 60:321–337.
18. Gallagher AR, Germino GG, Somlo S. Molecular advances in autosomal dominant polycystic kidney disease. Adv.Chronic.Kidney Dis. 2010; 17:118–130. [PubMed: 20219615]

19. Zhou J. Polycystins and primary cilia: primers for cell cycle progression. Annu.Rev.Physiol. 2009; 71:83–113. [PubMed: 19572811]
20. Patel V, et al. Acute kidney injury and aberrant planar cell polarity induce cyst formation in mice lacking renal cilia. Hum.Mol.Genet. 2008; 17:1578–1590. [PubMed: 18263895]
21. Nishio S, et al. Loss of oriented cell division does not initiate cyst formation. J.Am.Soc.Nephrol. 2010; 21:295–302. [PubMed: 19959710]
22. Shibazaki S, et al. Cyst formation and activation of the extracellular regulated kinase pathway after kidney specific inactivation of Pkd1. Hum.Mol.Genet. 2008; 17:1505–1516. [PubMed: 18263604]
23. Fedeles SV, et al. A genetic interaction network of five genes for human polycystic kidney and liver diseases defines polycystin-1 as the central determinant of cyst formation. Nat.Genet. 2011; 43:639–647. [PubMed: 21685914]
24. Piontek K, Menezes LF, Garcia-Gonzalez MA, Huso DL, Germino GG. A critical developmental switch defines the kinetics of kidney cyst formation after loss of Pkd1. Nat.Med. 2007; 13:1490–1495. [PubMed: 17965720]
25. Traykova-Brauch M, et al. An efficient and versatile system for acute and chronic modulation of renal tubular function in transgenic mice. Nat.Med. 2008; 14:979–984. [PubMed: 18724376]
26. Ruzankina Y, et al. Deletion of the developmentally essential gene ATR in adult mice leads to age-related phenotypes and stem cell loss. Cell Stem Cell. 2007; 1:113–126. [PubMed: 18371340]
27. Torres VE, Harris PC. Autosomal dominant polycystic kidney disease: the last 3 years. Kidney Int. 2009; 76:149–168. [PubMed: 19455193]
28. Boletta A. Emerging evidence of a link between the polycystins and the mTOR pathways. Pathogenetics. 2009; 2:6. [PubMed: 19863783]
29. Wallace DP. Cyclic AMP-mediated cyst expansion. Biochim Biophys Acta. 2011; 1812:1291–1300. [PubMed: 21118718]
30. Tao Y, Kim J, Schrier RW, Edelstein CL. Rapamycin markedly slows disease progression in a rat model of polycystic kidney disease. J Am Soc Nephrol. 2005; 16:46–51. [PubMed: 15563559]
31. Shillingford JM, et al. The mTOR pathway is regulated by polycystin-1, and its inhibition reverses renal cystogenesis in polycystic kidney disease. Proc.Natl.Acad.Sci.U.S.A. 2006; 103:5466–5471. [PubMed: 16567633]
32. Granot Z, et al. LKB1 regulates pancreatic beta cell size, polarity, and function. Cell Metab. 2009; 10:296–308. [PubMed: 19808022]
33. Walz G, et al. Everolimus in patients with autosomal dominant polycystic kidney disease. N.Engl.J Med. 2010; 363:830–840. [PubMed: 20581392]
34. Serra AL, et al. Sirolimus and kidney growth in autosomal dominant polycystic kidney disease. N.Engl.J Med. 2010; 363:820–829. [PubMed: 20581391]
35. Torres VE, et al. Effective treatment of an orthologous model of autosomal dominant polycystic kidney disease. Nat.Med. 2004; 10:363–364. [PubMed: 14991049]
36. Gattone VH, Wang X, Harris PC, Torres VE. Inhibition of renal cystic disease development and progression by a vasopressin V2 receptor antagonist. Nat.Med. 2003; 9:1323–1326. [PubMed: 14502283]
37. Torres VE. Cyclic AMP, at the hub of the cystic cycle. Kidney Int. 2004; 66:1283–1285. [PubMed: 15327429]
38. Calvet JP. Strategies to inhibit cyst formation in ADPKD. Clin.J.Am.Soc.Nephrol. 2008; 3:1205–1211. [PubMed: 18434615]
39. Sharma N, et al. Proximal tubule proliferation is insufficient to induce rapid cyst formation after cilia disruption. J Am Soc Nephrol. 2013; 24:456–464. [PubMed: 23411784]
40. Wong SY, et al. Primary cilia can both mediate and suppress Hedgehog pathway-dependent tumorigenesis. Nat.Med. 2009; 15:1055–1061. [PubMed: 19701205]
41. Han YG, et al. Dual and opposing roles of primary cilia in medulloblastoma development. Nat.Med. 2009; 15:1062–1065. [PubMed: 19701203]
42. Rohatgi R, Milenkovic L, Scott MP. Patched1 regulates hedgehog signaling at the primary cilium. Science. 2007; 317:372–376. [PubMed: 17641202]

43. Yoshiba S, et al. Cilia at the Node of Mouse Embryos Sense Fluid Flow for Left-Right Determination via Pkd2. Science. 2012
44. Goodrich LV, Milenkovic L, Higgins KM, Scott MP. Altered neural cell fates and medulloblastoma in mouse patched mutants. Science. 1997; 277:1109–1113. [PubMed: 9262482]
45. Wu G, et al. Somatic inactivation of Pkd2 results in polycystic kidney disease. Cell. 1998; 93:177–188. [PubMed: 9568711]
46. Marszalek JR, Ruiz-Lozano P, Roberts E, Chien KR, Goldstein LS. Situs inversus and embryonic ciliary morphogenesis defects in mouse mutants lacking the KIF3A subunit of kinesin-II. Proc Natl Acad Sci U S A. 1999; 96:5043–5048. [PubMed: 10220415]
47. Marszalek JR, et al. Genetic evidence for selective transport of opsin and arrestin by kinesin-II in mammalian photoreceptors. Cell. 2000; 102:175–187. [PubMed: 10943838]
48. Perl AK, Wert SE, Nagy A, Lobe CG, Whitsett JA. Early restriction of peripheral and proximal cell lineages during formation of the lung. Proc Natl Acad Sci U S A. 2002; 99:10482–10487. [PubMed: 12145322]
49. Shao X, Johnson JE, Richardson JA, Hiesberger T, Igarashi P. A minimal Ksp-cadherin promoter linked to a green fluorescent protein reporter gene exhibits tissue-specific expression in the developing kidney and genitourinary tract. J Am Soc Nephrol. 2002; 13:1824–1836. [PubMed: 12089378]
50. Muzumdar MD, Tasic B, Miyamichi K, Li L, Luo L. A global double-fluorescent Cre reporter mouse. Genesis. 2007; 45:593–605. [PubMed: 17868096]
51. Soriano P. Generalized lacZ expression with the ROSA26 Cre reporter strain [letter]. Nat.Genet. 1999; 21:70–71. [PubMed: 9916792]
52. Zou Z, et al. Linking receptor-mediated endocytosis and cell signaling: evidence for regulated intramembrane proteolysis of megalin in proximal tubule. J Biol Chem. 2004; 279:34302–34310. [PubMed: 15180987]
53. Cai Y, et al. Identification and characterization of polycystin-2, the PKD2 gene product. J.Biol.Chem. 1999; 274:28557–28565. [PubMed: 10497221]
54. Caspary T, Larkins CE, Anderson KV. The graded response to Sonic Hedgehog depends on cilia architecture. Dev Cell. 2007; 12:767–778. [PubMed: 17488627]
55. Saifudeen Z, Marks J, Du H, El-Dahr SS. Spatial repression of PCNA by p53 during kidney development. Am J Physiol Renal Physiol. 2002; 283:F727–733. [PubMed: 12217864]

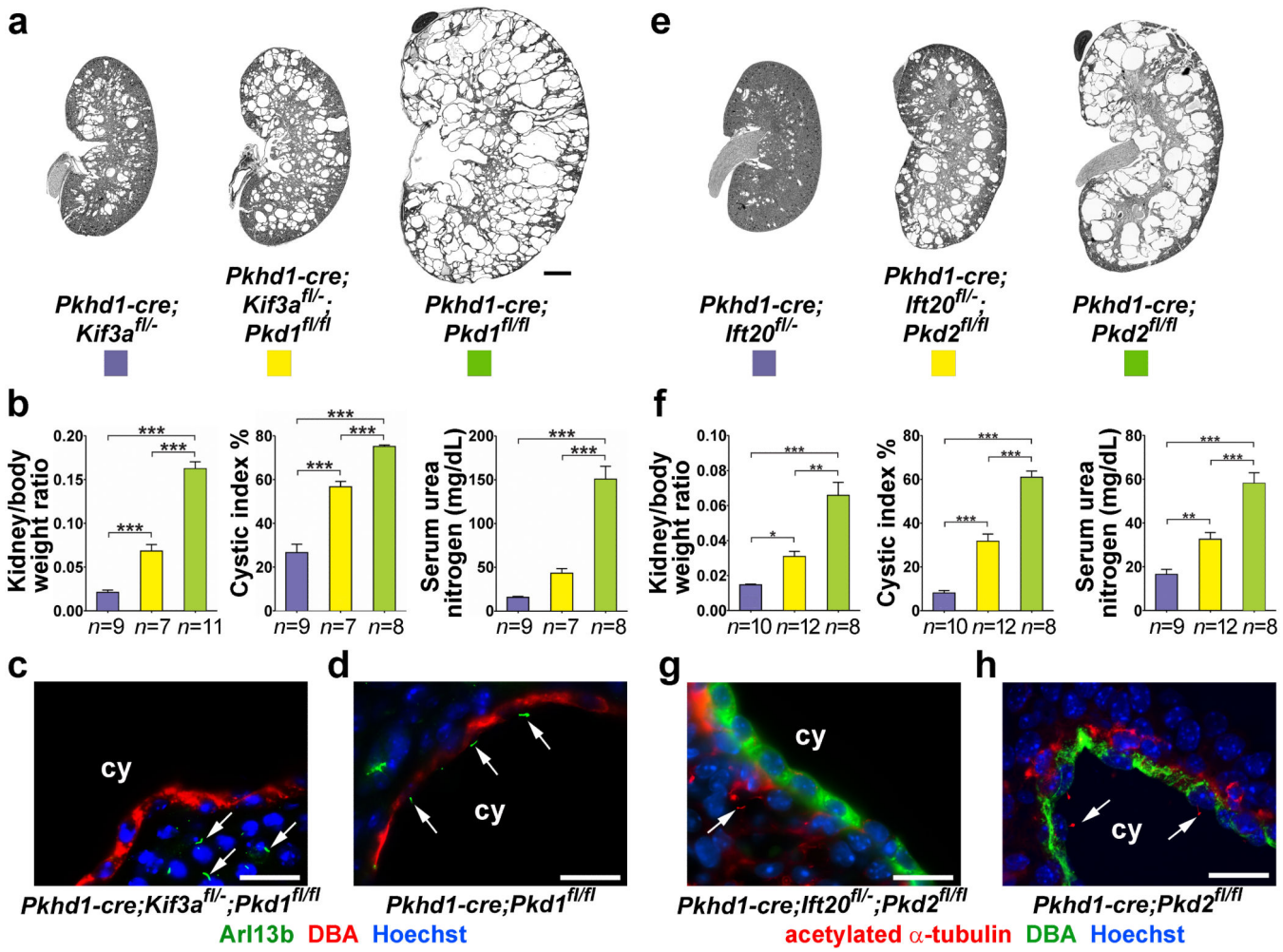

Figure 1. Concomitant ablation of cilia ameliorates progression of ADPKD

Double inactivation of cilia and polycystins reduces cyst formation irrespective of the polycystin gene involved (*Pkd1*, **a-d**, *Pkd2*, **e-h**), the gene targeted for cilia ablation (*Kif3a*, **a-d**, *Ift20*, **e-h**). Representative images (**a**, **e**) and aggregate quantitative data (**b**, **f**) of kidney-to-body weight ratio, percent cystic area (cystic index) and serum urea nitrogen with the indicated genotypes. Immunohistochemistry showing (**c, g**) absence of cilia in cilia-polycystin double mutants and (**d, h**) presence of cilia in polycystin-only single mutants. Mice were examined at P24. Arrows indicate cilia. The color squares represent the respective genotypes in the histograms. The numbers of animals (*n*) in each group are indicated below the histogram bars. Multiple group comparisons were performed using one-way ANOVA followed by Tukey's multiple comparison test and are presented as the mean ± SEM (***, P<0.001; **, P<0.01; *, P<0.05). Scale bar, 2 mm for **a**, **e**; 20 μm for **c**, **d**, **g**, **h**.

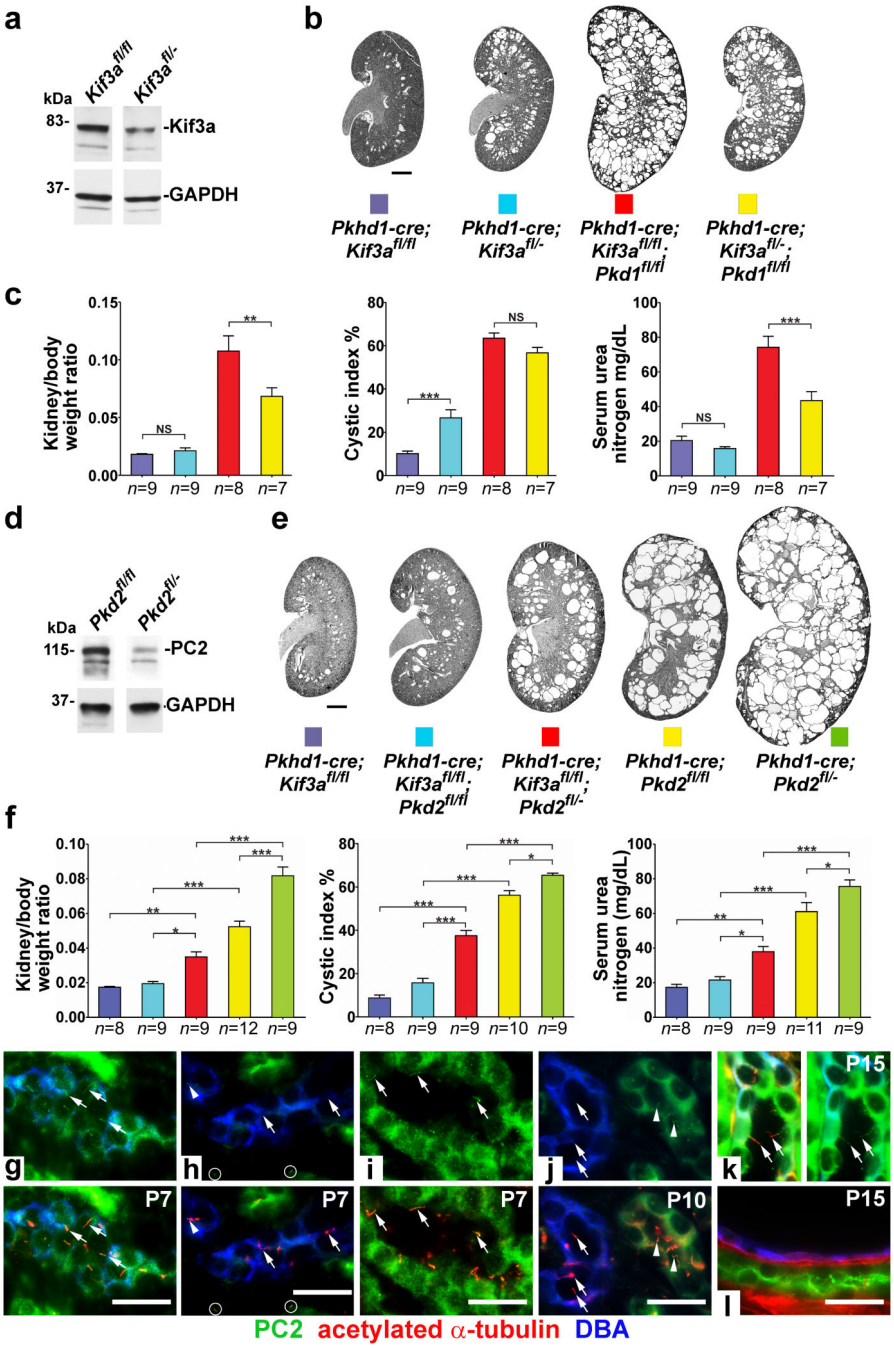

Figure 2. Polycystic disease severity is directly related to the length of time between polycystin loss and involution of cilia

Extending the time interval between loss of polycystins and the subsequent involution of cilia by varying the gene dosage of *Kif3a* (**a-c**) or *Pkd2* (**d-f**) results in increased cyst growth. Immunoblotting shows higher steady state levels of the respective proteins at P10 (**a**) in $Kif3a^{fl/fl}$ compared to $Kif3a^{fl/-}$ and (**d**) in $Pkd2^{fl/fl}$ compared to $Pkd2^{fl/-}$ kidneys. (**b, e**) Representative images and (**c, f**,) aggregate quantitative data for kidneys with the indicated genotypes at P24. Cilia in $Kif3a^{fl/fl}$ kidneys disappear later (P14) than in $Kif3a^{fl/-}$ kidneys

(P11) resulting in more severe polycystic disease in *Kif3a*$^{fl/fl}$;*Pkd1*$^{fl/fl}$ double mutants (red vs. yellow). Lower initial levels of PC2 in *Pkd2*$^{fl/-}$ mice result in earlier disappearance of PC2 and increased disease severity in cilia-PC2 double mutants compared (red) to *Pkd2*$^{fl/fl}$ double mutants (blue). The numbers of animals (*n*) in each group are indicated below the histogram bars. Multiple group comparisons were performed using one-way ANOVA followed by Tukey's multiple comparison test and are presented as the mean ± SEM (***, P<0.001; **, P<0.01; *, P<0.05; NS, not significant). It should be noted that *Pkhd1-cre; Kif3a*$^{fl/-}$ (blue) and *Pkhd1-cre; Kif3a*$^{fl/-}$; *Pkd1*$^{fl/fl}$ (yellow) in **b**, **c** are the same mice as in Fig. 1a, b compared to the respective aged matched *Kif3a*$^{fl/fl}$ mice; although analyzed by ANOVA, only the relevant comparisons are shown. (**g-l**) Immunofluorescence studies showing the earlier disappearance of PC2 and subsequent involution of cilia. (**g**) Wild type P7 mouse kidney sections showing cilia (arrows) marked by acetylated α-tubulin (red, lower panel) in collecting ducts (blue) expressing PC2 (green, upper panel); (**k**), wild type kidney at P15. Collecting ducts at P7 in *Pkhd1-cre; Kif3a*$^{fl/fl}$; *Pkd2*$^{fl/fl}$ double mutant mice (**h**) show that most cilia (arrows, bottom panel) no longer express PC2 (top panel) although low level expression is occasionally observed in a few cilia (arrowhead). Non-collecting duct segments that do not express Cre in the same tissue sections continue to express PC2 in cilia (**i**; circles in **h**). At P10 (**j**), collecting duct cilia (arrows, lower) are completely devoid of PC2 (arrows, upper) while adjacent tubules where Cre is not active continue to express PC2 in cilia (arrowheads). By P15 (**l**), collecting ducts no longer have cilia. Scale bar, 2 mm for **b**, **e**; 20 μm for **g-l**.

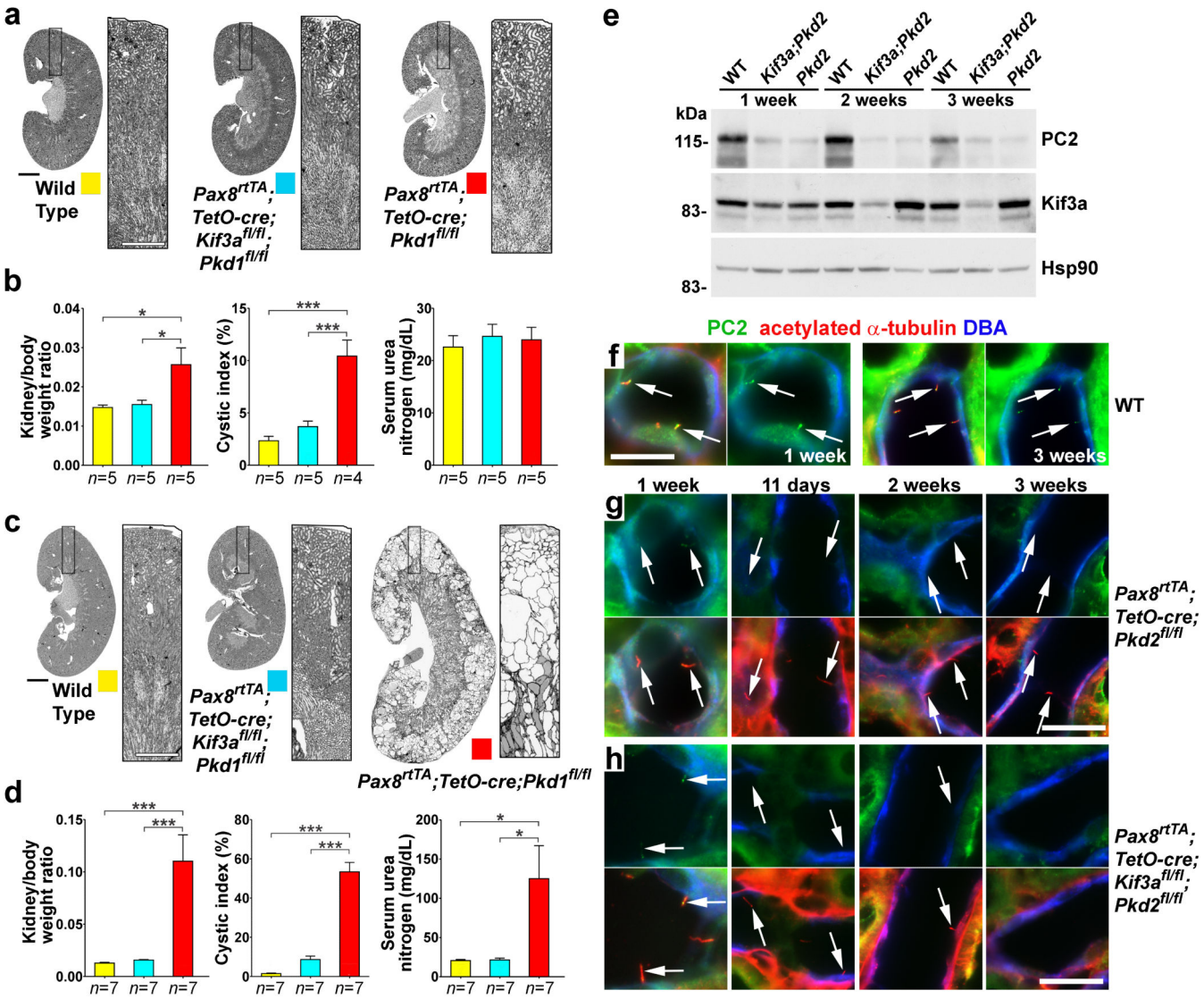

Figure 3. Disruption of cilia reduces kidney cyst growth in adult onset ADPKD

Representative images of kidneys with the specified genotypes at (**a**) 8 weeks and (**c**) 14 weeks after the start of induction (mice aged 12 and 18 weeks, respectively); boxed regions are enlarged in the panel to the right of the kidney image. (**b**, **d**) Aggregate analysis of kidney weight-to-body weight ratio, cystic index and serum urea nitrogen at (**b**) 8 weeks and (**d**) 14 weeks after the start of induction. The color squares represent the respective genotypes in the histograms. The numbers of animals (*n*) in each group are indicated below the histogram bars. Multiple group comparisons were performed using one-way ANOVA followed by Tukey's multiple comparison test and are presented as the mean ± SEM (***, P<0.001; *, P<0.05). (**e**) Immunoblot analysis of PC2 and Kif3a protein levels in control, *Pax8^{rtTA}; TetO-cre; Kif3a$^{fl/fl}$; Pkd2$^{fl/fl}$* (*Kif3a;Pkd2*) and *Pax8^{rtTA}; TetO-cre; Pkd2$^{fl/fl}$* (*Pkd2*) mice at 1, 2 and 3 weeks after the start of doxycycline induction. PC2 expression is already markedly reduced at 1 week after the start of induction in double knockouts whereas comparable reduction in Kif3a is observed at 2 weeks after starting induction; HSP90 was

used as loading control. (**f-h**) Immunofluorescence using anti-PC2 (green), anti-acetylated α-tubulin (red) and DBA (pseudo-blue) showing the relative timing of loss of PC2 and involution of cilia in adult inactivation models. (**f**) Control kidney express PC2 in cilia at 1 and 3 weeks. Left panels, merged image; right panel, PC2. (**g**) Pkd2-only mutant kidneys show loss of PC2 by 11 days after the start of doxycycline induction. (**h**) Kif3a;Pkd2 double mutant kidneys show that cilia devoid of PC2 are present at 11 days following start of doxycycline. Cilia persist at 2 weeks following start of doxycycline, although in reduced numbers. Cilia are totally absent by 3 weeks following the start of doxycycline. (**g, h**) Top panels show PC2 and bottom panels show merged image. Arrows, cilia. Scale bars: **a**, **c**, 2 mm; **f-h**, 20 μm.

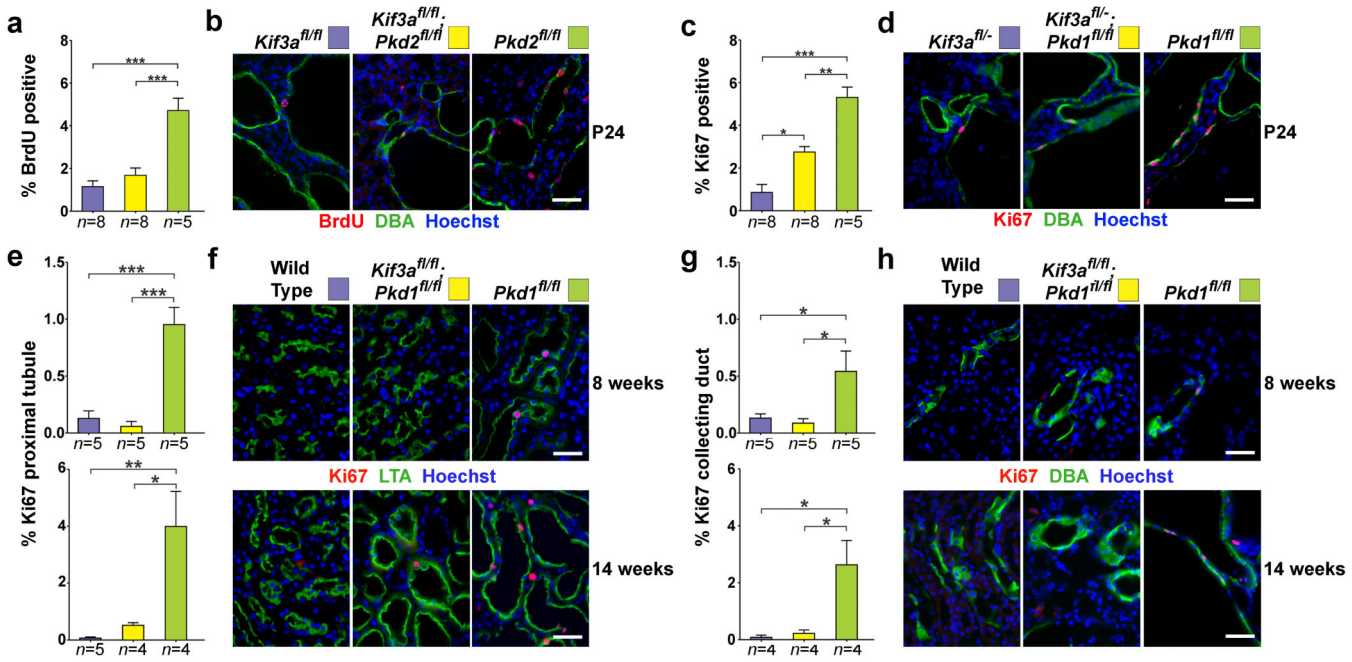

Figure 4. Loss of cilia in ADPKD suppresses cyst growth through reduction of cyst cell proliferation

(**a**) Aggregate quantitative analysis of the percentage of BrdU-positive nuclei and (**c**) Ki67 positive nuclei and the respective representative images (**b, d**) at P24 in an allelic series of the specified genotypes using inactivation by *Pkhd1-cre*. Quantitation of proliferation was determined by counting the number of BrdU or Ki67 positive nuclei amongst at least 1000 DBA positive cells in each mouse. Aggregate quantitative data (**e, g**) and representative images (**f, h**) with the indicated genotypes combined with *Pax8^{rtTA}; TetO-cre* at 8 and 14 weeks after the start of doxycycline induction (respective ages, 12 and 18 weeks). Segment-specific adult model proliferation rates were determined for proximal tubules (**e, f**) and collecting ducts (**g, h**). The color squares in **b**, **d**, **f** and **h** correspond to the respective genotypes in the histograms in **a**, **c**, **e** and **g**. The numbers of animals (*n*) in each group are indicated below the histogram bars. Multiple group comparisons were performed using one-way ANOVA followed by Tukey's multiple comparison test and are presented as the mean ± SEM (***, P<0.001; **, P<0.01; *, P<0.05). Scale bar, 40 μm.

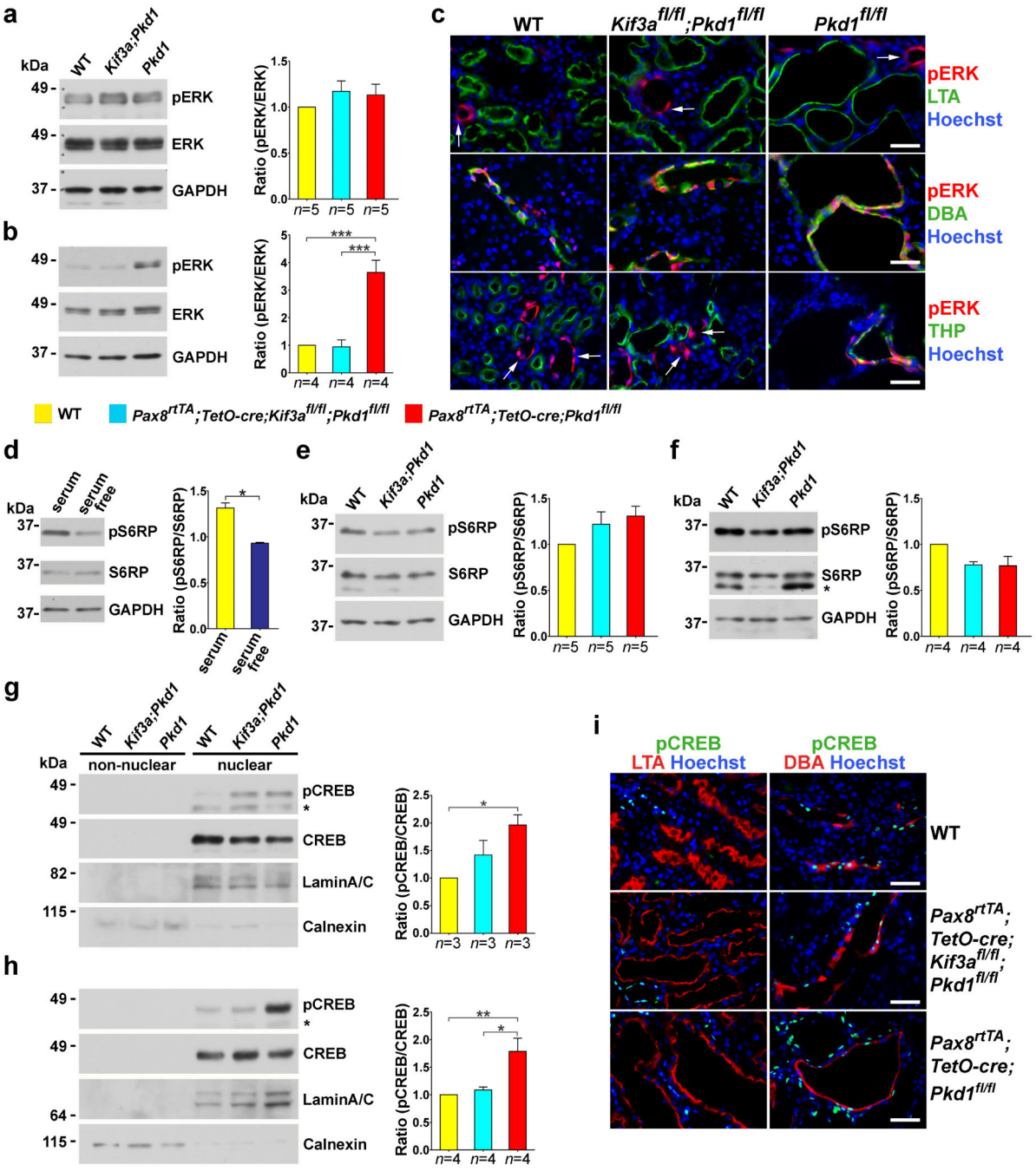

Figure 5. ***In vivo*** **MAPK/ERK, mTOR and cAMP signaling as a function of cilia ablation in ADPKD**

(**a-c**) *In vivo* phosphorylation of ERK1/2 (pERK) in wild type, *Pax8*^{rtTA}*; TetO-cre; Kif3a*$^{fl/fl}$*; Pkd1*$^{fl/fl}$ and *Pax8*^{rtTA}*; TetO-cre; Pkd1*$^{fl/fl}$ at (**a**) 8 weeks and (**b, c**) 14 weeks after the start of induction with doxycycline. Representative immunoblots and aggregate densitometric quantitation of kidney lysates show that pERK is not increased in any genotype at 8 weeks (**a**) and is elevated at 14 weeks (**b**) only in the cystic *Pkd1* single knockouts. (**c**) Immunohistochemical evidence of pERK expression at 14 weeks after

induction is commonly found in CD irrespective of genotype; it is ubiquitously absent from proximal tubule irrespective of the extent of cyst formation; and it appears in thick ascending loop of Henle only in *Pax8^{rtTA}; TetO-cre; Pkd1$^{fl/fl}$* cystic mice. The increase in pERK in kidney lysates at 14 weeks is at least partly the result of increased cell mass of DBA positive CD cells comprising cysts. Arrows show positive pERK expression in segments other than proximal tubule (top panels) and thick ascending loop of Henle (bottom panels). (**d-f**) Phosphorylation of the mTOR pathway activation substrate S6RP. (**d**) Serum starvation of cultured cells is known to downregulate mTOR and result in decreased pS6RP, confirming the specificity of the antibody (n=4 for each group). Comparisons were performed using Mann-Whitney test and are presented as the mean ± SEM (*, P<0.05). (**e, f**) Representative immunoblots and aggregate densitometric quantitation of kidney lysates show no change in pS6RP irrespective of genotype and extent of cyst formation at **(e**) 8 weeks and (**f**) 14 weeks after the start of Cre induction suggesting that the mTOR pathway is not activated in these adult models. (*) in **f**, non-specific band. (**g-i**) *In vivo* cAMP-dependent phosphorylation of CREB (pCREB) at (**g**) 8 weeks and (**h, i**) 14 weeks after the start of Cre induction. Representative immunoblots and aggregate densitometric quantitation showing nuclear and non-nuclear fractions of kidney tissue lysates. pCREB activity is elevated at (**g**) 6 weeks and (**h**) 12 weeks only in *Pax8^{rtTA}; TetO-cre; Pkd1$^{fl/fl}$* cystic mice. (*) in **g**, **h** denote the phosphorylated form of cyclic AMP-dependent transcription factor ATF-1 that is known to cross react with the pCREB antibody. LaminA/C and calnexin are used to show relative nuclear enrichment and control loading. (**i**) Immunohistochemistry of pCREB expression at 14 weeks after induction shows nuclear staining in CD that is markedly increased in *Pax8^{rtTA}; TetO-cre; Pkd1$^{fl/fl}$* cystic mice. pCREB is completely absent from LTA positive PT irrespective of genotype or degree of cystic transformation. *Pax8^{rtTA}; TetO-cre; Pkd1$^{fl/fl}$* cystic mice also show increased pCREB in nuclei of segments that are negative for DBA (lower right panel). The color squares in the legend correspond to the respective genotypes in the histograms. The numbers of animals (n) in each group are indicated below the histogram bars. Multiple group comparisons were performed using one-way ANOVA followed by Tukey's multiple comparison test and are presented as the mean ± SEM except as indicated above (***, P<0.001; **, P<0.01; *, P<0.05). Scale bar, 40 μm.